NUKLEONIKA 2016;61(2):219–223
doi: 10.1515/nuka-2016-0037

ORIGINAL PAPER - REGULAR PAPER

DE GRUYTER OPEN

Imaging of hypoxia in small animals with ^{18}F fluoromisonidasole*

Krzysztof Kilian, Zbigniew Rogulski, Łukasz Cheda, Agnieszka Drzał, Marina Gerszewska, Michał Cudny, Martyna Elas

Abstract. A method of automated synthesis of [^{18}F]fluoromisonidazole ([^{18}F]FMISO) for application in preclinical studies on small animals was presented. A remote-controlled synthesizer Synthra RN_{plus} was used for nucleophilic substitution of NITTP (1-(2′-nitro-1′-imidazolyl)-2-O-tetrahydropyranyl-3-O-toluenesulfonyl-propanediol) with ^{18}F anion. Labeling of 5 mg of precursor was performed in anhydrous acetonitrile at 100°C for 10 min, and the hydrolysis with HCl was performed at 100°C for 5 min. Final purification was done with high-performance liquid chromatography (HPLC) and the radiochemical purity of radiotracer was higher than 99%. Proposed [^{18}F]FMISO synthesis was used as a reliable tool in studies on hypoxia in Lewis lung carcinoma (LLC) in mouse models.

Key words: ^{18}F-fluoromisonidazole • radiopharmaceuticals • hypoxia imaging

K. Kilian✉
Heavy Ion Laboratory,
University of Warsaw,
5A Pasteura Str., 02-093 Warsaw, Poland,
Tel.: +48 22 55 46 214,
E-mail: kilian@slcj.uw.edu.pl

Z. Rogulski, Ł. Cheda
Faculty of Chemistry,
University of Warsaw,
1 Pasteura Str., 02-093 Warsaw, Poland

A. Drzał, M. Elas
Faculty of Biochemistry, Biophysics and Biotechnology,
Jagiellonian University,
7 Gronostajowa Str., 30-387 Krakow, Poland

M. Gerszewska, M. Cudny
Faculty of Physics,
University of Warsaw,
5 Pasteura Str., 02-093 Warsaw, Poland

Received: 30 September 2015
Accepted: 9 March 2016

Introduction

Hypoxia defines a pathological condition where oxygen is delivered to the tissue in insufficient quantities, which is the result of impaired oxygen transport mechanism. Hypoxic conditions may have the features of the pathological process, e.g. during the development of uncontrolled proliferative lesions [1, 2]. Regardless of the stage of the cancer, tumor hypoxia is considered to be unfavorable prognostic factor [3]. Hypoxic cells exhibit greater resistance to all therapeutic modes [4] and provide higher probability of metastasis and recurrence [5]. Therefore, the determination of the level and spatial distribution of hypoxia in tumor cells is an important diagnostic problem.

In recent years, the molecular imaging methods, in particular positron emission tomography (PET), proved the effectiveness in the diagnosis of hypoxic conditions.

As a radiopharmaceutical for the diagnosis of hypoxia, a complex of radioactive copper-64 ($t_{1/2}$ = 12.7 h) with a neutral lipophilic molecule ATSM (diacetyl-bis(N4-methylthiosemicarbazone)) was successfully applied [6]. ^{64}Cu(II)-ATSM was reduced in hypoxic *in vivo* conditions and converted

* This paper is based on a lecture given at the Warsaw Medical Physics Meeting held in Warsaw, Poland, on 14–15 May 2015.

into an anion [Cu(I) ATSM]$^{-}$, which was trapped inside the cells, particularly in poorly vascularized areas in the state of cell cycle arrest. ^{64}Cu-ATSM was an excellent marker for live cells in a hypoxic state but did not accumulate in the areas of necrosis, thus the amount of captured ^{64}Cu-ATSM by tumor cells was inversely proportional to the chance of survival and lifetime without metastasis or recurrence [7].

The most widely used marker for imaging hypoxic conditions is [^{18}F]fluoromisonidazole ([^{18}F]FMISO) labeled with fluorine-18 ($t_{1/2}$ = 110 min), routinely and worldwide manufactured isotope for neuro- and oncological diagnostics. As other molecules containing 2-nitroimidazole moiety is reduced in hypoxic cells, whereby it is used as an indicator of the oxygen concentration in tumor cells [8]. Imaging with [^{18}F]FMISO takes 20–30 min (whole body scan) and is performed 2–4 hours after administration. Because the [^{18}F]FMISO is not captured by the areas covered by necrosis, it requires the presence of living cells in hypoxic pO_2 level below 10 mmHg [9]. [^{18}F]FMISO increased its clinical significance when noninvasive assessment of hypoxia has been applied for detecting the differences between various types of tumors and delineation of hypoxic areas in radiation therapy planning.

In preclinical research, [^{18}F]FMISO examination started to be a tool for phenotypes characterization [10], monitoring of anticancer treatments [11], response evaluation [12], and molecular backgrounds of spontaneous tumors [13].

This paper describes an application of [^{18}F]FMISO for the preclinical studies on small animals. The scope of this study was to synthesize [^{18}F]FMISO in a number of consecutive runs using fluorine from target flushing after the commercial manufacturing of fluorodeoxyglucose ([^{18}F]FDG) and to prove the quality of manufactured radiopharmaceuticals, as a proof of concept in studies on hypoxia in Lewis lung carcinoma (LLC) in mouse models.

Materials and methods

[^{18}F]FMISO synthesis

[^{18}F]FMISO was synthesized by nucleophilic fluorination of NITTP (1-(2′-nitro-1′-imidazolyl)--2-O-tetrahydropyranyl-3-O-toluenesulfonyl--propanediol) with acidic hydrolysis. Cyclotron GE PETtrace 840 with high-yield niobium target (General Electric, Uppsala, Sweden) was the source of anionic fluorine. Standard produced activity in the ^{18}O(p,n)^{18}F reaction with a 16.5-MeV proton beam at 40–45 μA was 4.0 ± 0.2 Ci (140.6–155.4 GBq) after 120 min of irradiation, and this was used for commercial ^{18}FDG synthesis.

For animal studies, residual activity (4.0–6.0 GBq of fluorine in 2.2 ml of H_2O) from flushing the target after commercial ^{18}FDG synthesis was transferred to the Synthra RN_{plus} unit (Synthra, Germany), where the [^{18}F]FMISO synthesis and purification were performed (Fig. 1). Precursor NITTP in 5 mg portions and Kryptofix in acetonitrile were obtained from ABX (Radeberg, Germany); other reagents such as potassium carbonate p.a., anhydrous acetonitrile (high-performance liquid chromatography (HPLC) grade), ethanol (HPLC grade), and hydrochloric acid p.a. were obtained from Avantor Chemicals (Gliwice, Poland).

Identification and quality control

Identity of manufactured [^{18}F]FMISO was confirmed by comparison of retention time to the certified reference standard (CRS) of main compound (ABX, Radeberg, Germany).

Radiochemical purity was performed with chromatography system Shimadzu AD20 with UV-Vis (ultraviolet-visible) and radiometric detector (GabiStar, Raytest, Germany). Twenty microliters

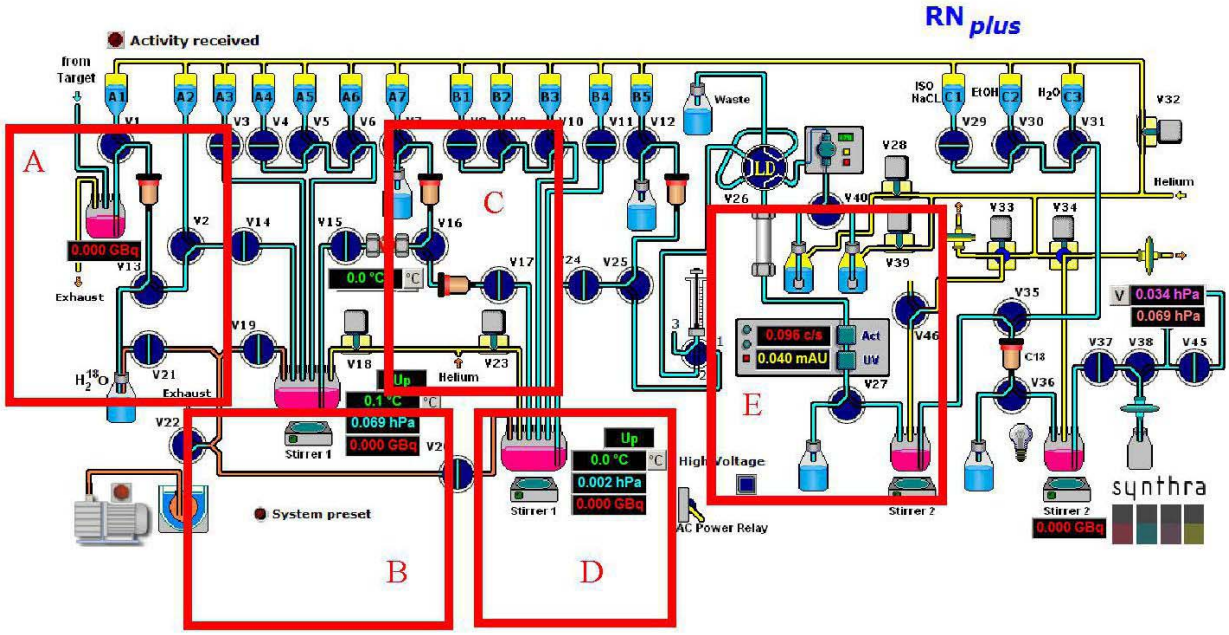

Fig. 1. Control panel and scheme of Synthra RN_{Plus} module. (A) ^{18}F trapping and separation from target; (B) ^{18}F labeling of precursor; (C) purification of intermediate product; (D) acidic hydrolysis; (E) HPLC purification and final formulation.

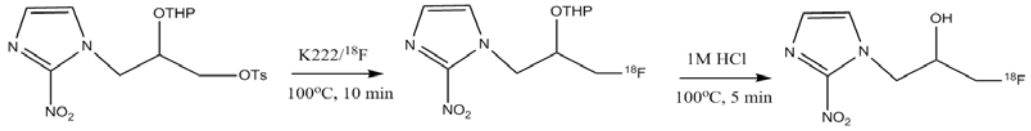

Fig. 2. Synthesis of [^{18}F]FMISO.

of sample was injected via manual multiport valve. The separation was done on Phenomenex Gemini C18 column (150 mm × 4.0 mm i.d., 10 μm), with 95:5 H_2O:EtOH as a mobile phase and 1 mL/min flow rate.

Other identification tests, half-life measurements, pH, residual solvents, and radionuclidic purity were performed as described earlier for [^{18}F]FDG [14].

Animals and tumor model

LLC cells were grown at 37°C in a humidified atmosphere of 5% CO_2/95% air in RPMI 1640 containing 10% heat-inactivated fetal bovine serum plus penicillin-streptomycin under sterile tissue culture conditions. C57BL/6JOlaHsd, N = 10 female mice of 8–10 weeks of age and about 20 g of each were originally obtained from the animal breeding facility at the Faculty of Biochemistry, Biophysics and Biotechnology of the Jagiellonian University (Cracow, Poland). All the experimental procedures were approved by the First Local Ethic Committee of the Jagiellonian University (Permission Nos. 107/2013 and 91/2014). Mice were kept under constant conditions of 12/12 light cycle, humidity of 60%, and temperature of about 23°C. Standard laboratory diet with free access to drinking water were given in community cages. For each mouse, 0.5×10^6 LLC cells, suspended in 100 μL of PBS, was injected intradermally into the right hind limb. The tumors became visible in 4–6 days after implantation. When their size (greatest diameter) were about 5 mm, mice were transported in cages specially prepared for this purpose to Biological and Chemical Research Centre of the University of Warsaw. Positron emission tomography-computed tomography (PET/CT) measurements were performed after minimum 24 hours of acclimation after travel.

PET/CT measurements

Experiments were performed on Albira PET/SPECT/CT Preclinical Imaging System (Bruker, Germany). Before measurements, mice were anesthetized with 2% isoflurane (Aerrane, Baxter Polska Sp. z o.o., Poland) in oxygen delivered through a nose cone and place on the heating pad. Thin cannula connected with a pressure equalizing (PE) tube (PE 50) of 15 cm long filled with saline was placed in tail vein. Prepared mice were placed in the supine position in the imager with the use of the animal bed, and 10–15 MBq [^{18}F]FMISO was administered i.v. through tail vein cannula. Isoflurane anesthesia were maintained through entire radiopharmaceutical uptake and image acquisition. Respiration was monitored with pressure pad connected to differential pressure transducers for low-range pressure monitoring (Biopac MP150 Acquisition System) during entire PET/CT examination and regulated by changing isoflurane concentration. PET scans were performed 120 min after injection. Emission data were collected for 1, 5, and 10 min. Spatial resolution of PET measurements was 1.1 mm. The scan parameters were set as follow: tube voltage was 45 kVp, tube current was 400 μA, and number of projections was 400. Minimal resolution of CT was 90 μm. The PET and CT images were fused using a PMOD software. Because the mouse remains in the same position on the bed for both PET and CT acquisitions, the software module can use the positional information to fuse and coregister the PET and CT data.

Results and discussion

Synthesis

[^{18}F]FMISO was synthetized by direct nucleophilic [^{18}F]fluorination of NITTP (Fig. 2) in commercially available module Synthra RN_{Plus}. As a source of fluorine, the water after first flushing of the irradiated target has been used. In standard conditions, activities in range 4.0–6.0 GBq were obtained and directed to the synthesis unit.

First, the solution was passed through an ion-exchange column (Chromafix 731876 PS-HCO_3^-), which trapped ^{18}F anions. Then, fluoride was eluted to the reaction vessel with a mixture of potassium carbonate and Kryptofix 2.2.2. Water was removed by azeotropic distillation with anhydrous acetonitrile and ^{18}F reacted with 5 mg of NITTP. Reaction mixture was purified on C18 SPE column (Chromafix 731805 (C18EC)) and further fluorinated precursor was eluted with ethanol to the second reactor, where 1.5 mL of 1 M hydrochloric acid was added for hydrolysis (5 min, 100°C).

After acidic hydrolysis, the solution was purified with built-in HPLC on C18-RP (Phenomenex Gemini C18 250 mm × 10 mm × 7 μm). This method of separation was confirmed as the most effective purification method [15]. To receive high specific activity, the modification of synthesis module was done to enable the collection of the fraction with highest activity of final product. The 1-mL portion of the most concentrated product at the output form HPLC column was cut-off by valve V27 and directly delivered with helium stream to the final product vial, after passing through the 0.22-μm sterile filter. Finally, it was formulated with saline (0.9% w/v) and dispensed in manual module μDDS-A (Tema Sinergie, Italy).

Radiochemical yield was 35.1 ± 1.2% (not corrected); total synthesis time including activity and final product transfer was 50–52 min, which is

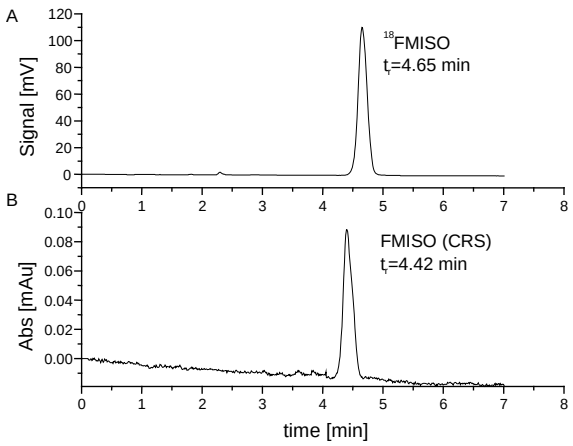

Fig. 3. Radiochemical purity and identity for [^{18}F]FMISO. (a) Radiochromatogram compared with (b) UV-Vis (254 nm) reference.

comparable to recently published papers [15, 16], taking into consideration yield dependency on initial precursor mass [17].

The labeling reaction was followed with preparative HPLC, ensuring good separation of final product from impurities and the radiochemical purity >99%. On the basis of the starting activity of 4.0–6.0 GBq, 1.2–1.7 GBq of product with specific activity of 200–250 MBq/mL was obtained, which was sufficient for the injection of several animals in standard imaging mode.

Quality control

^{18}F was identified by recording the principal γ-peak at 511.5 ± 0.3 keV and determining the half-life (108.8 ± 0.3 min). The presence of any peaks with an energy different from 511 keV was checked and, except signals coming from Pb-X-rays (range 70–80 keV), none was found. That confirmed a better than 99.9% radionuclidic purity. Then the sample was left for 24 h to decay and again impurities were tested with no significant peaks, except residual activity of ^{18}F.

[^{18}F]FMISO was identified, comparing the retention times of standards, observed in the reference chromatogram with retention time of the principal signal in the radiochromatogram (Fig. 3). Recorded retention times were 4.42 min for the standard and 4.65 min for the principal peak in radiochromatogram.

Radiochemical purity was determined by HPLC with radiometric detection, where the peak of [^{18}F]FMISO was observed at 4.65 min, with no other signals recorded (Fig. 3b). The average content of [^{18}F]FMISO was higher than 99%. Six consecutive runs were analyzed in triplicate each. Osmolality of formulated product was 310 mOsm/kg; pH ranged 6.5–7.4.

Imaging

The synthesized and HPLC-purified [^{18}F]FMISO was used for PET imaging in a mouse model carrying LLC tumor. For comparison, the same mouse

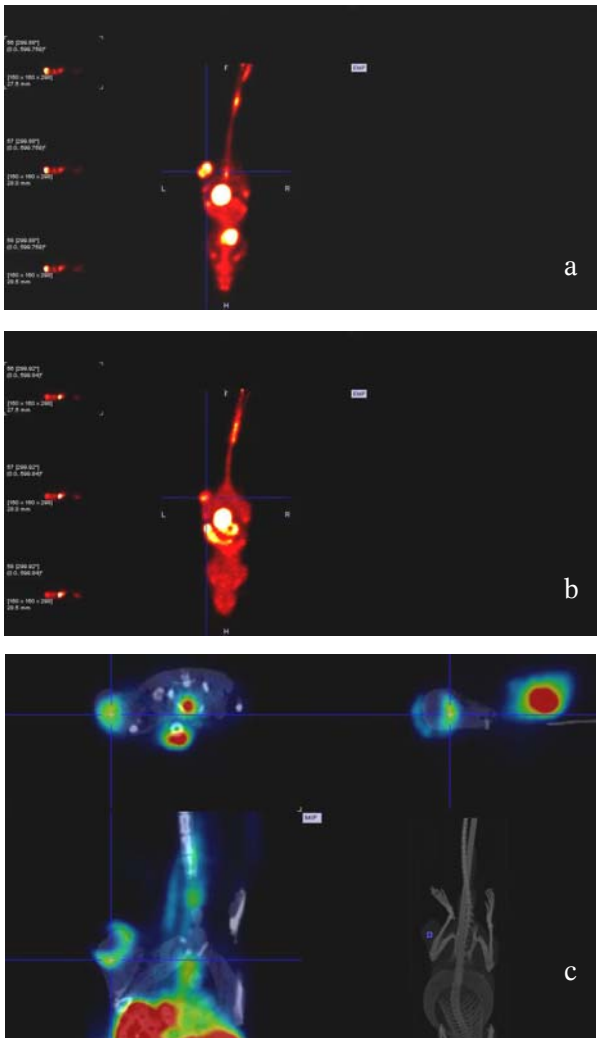

Fig. 4. *In vivo* imaging of a mouse carrying LLC tumor with [^{18}F]FDG (a) and [^{18}F]FMISO (b) with detailed distribution of hypoxia with [^{18}F]FMISO in tumor (c).

was also imaged with [^{18}F]FDG. The results show a difference in the distribution of [^{18}F]FDG and [^{18}F]FMISO in the body (Fig. 4).

The physiological uptake of glucose is located in the heart and bladder; in the case of [^{18}F]FMISO, tracer is accumulated in the intestine and bladder. It confirms other studies in which [^{18}F]FMISO had physiological affinity to the gastrointestinal tract [11]. In the stomach and intestine, high absorption was observed 30 min after the injection, whereas in the kidney, uptake increased 30 min after injection and remained in bladder at a high level to 120 min. The visible difference in the structure of imaged cancer with [^{18}F]FDG and [^{18}F]FMISO is observed – for the first tracer, tumor area is spherical and [^{18}F]FMISO is accumulated in two separated sites. While [^{18}F]FMISO was accumulated in relatively hypoxic areas of the tumor, ^{18}[F]FDG was preferentially taken up by metabolically active tumor regions. The reason for the differences in structure of imaged tumor depends on the uptake mechanism of the marker [18], where the uptake of [^{18}F]FDG in the tumor is caused by increased glucose metabolism and [^{18}F]FMISO is the result of the presence of hypoxic areas of the tumor tissue.

Conclusions

Synthesis of [^{18}F]FMISO using 5 mg of precursor NITTP offered reliable manufacturing of good yield and high-purity radiopharmaceutical. The modifications to the synthesis unit allowed to receive sufficient activity to perform PET experiments in animal subjects. Produced [^{18}F]FMISO was used as a reliable tool in studies on hypoxia in LLC in mouse models.

Acknowledgments. Heavy Ion Laboratory gratefully acknowledges funding for the equipment from the Ministry of Health and from the European Regional Development Fund under the Innovative Economy Programme (POIG.02.02.00-14-024/08-00) project: Center of Preclinical Studies and Technology (CePT).

References

1. Bristow, R. G., & Hill, R. P. (2008). Hypoxia and metabolism: Hypoxia, DNA repair and genetic instability. *Nat. Rev. Cancer*, *8,* 180–192.
2. Zhang, J., Cao, J., Ma, S., Dong, R., Meng, W., Ying, M., Weng, Q., Chen, Z., Ma, J., Fang, Q., He, Q., & Yang, B. (2014). Tumor hypoxia enhances non-small cell lung cancer metastasis by selectively promoting macrophage M2 polarization through the activation of ERK signaling. *Oncotarget*, *5*(20), 9664–9677.
3. Ackerman, D., & Simon, M. C. (2014). Hypoxia, lipids, and cancer: surviving the harsh tumor microenvironment. *Trends Cell. Biol., 24*(8), 472–477.
4. Brown, J. M. (2007). Tumor hypoxia in cancer therapy. H. Sies, & B. Brune (Eds.) *Methods in enzymolology. Vol. 435* (pp. 297–321). Academic Press.
5. Nagelkerke, A., Bussink, J., Mujcic, H., Wouters, B. G., Lehmann, S., Sweep, F. C. G. J., & Span, P. N. (2013). Hypoxia stimulates migration of breast cancer cells via the PERK/ATF4/LAMP3-arm of the unfolded protein response. *Breast Cancer Res*., *15*, R2(13pp).
6. Weeks, A. J., Paul, R. L., Marsden, P. K., Blower, P. J., & Lloyd, D. R. (2010). Radiobiological effects of hypoxia dependent uptake of 64Cu-ATSM: enhanced DNA damage and cytotoxicity in hypoxic cells. *Eur. J. Nucl. Med. Mol. Imaging*, *37*, 330–338.
7. Mees, G., Dierckx, R., Vangestel, Ch., & Van de Wiele, Ch. (2009). Molecular imaging of hypoxia with radiolabelled agents. *Eur. J. Nucl. Med. Mol. Imaging*, *36*, 1675–1680.
8. Peeters, S. G., Zegers, C. M., Lieuwes, N. G., van Elmpt, W., Eriksson, J., van Dongen, G. A., Dubois, L., & Lambin, P. (2015). A comparative study of the hypoxia PET tracers [18F]HX4, [18F]FAZA, and [18F]FMISO in a preclinical tumor model. *Int. J. Radiat. Oncol. Biol. Phys*. *1, 91*(2), 351–359.
9. Lin, A., & Hahn, S. M. (2012). Hypoxia imaging markers and applications for radiation treatment planning. *Semin. Nucl. Med*., *42*, 343–352.
10. Campanile, C., Arlt, M. J. E., Krämer, S. D., Honer, M., Gvozdenovic, A., Brennecke, P., Fischer, C. A., Sabile, A. A., Müller, A., Ametamey, S. A., Born, W., Schibli, R., & Fuchs, B. (2013). Characterization of different osteosarcoma phenotypes by PET imaging in preclinical animal models. *J. Nucl. Med*., *54*(8), 1362–1368.
11. Thézé, B., Bernards, N., Beynel, A., Bouet, S., Kuhnast, B., Buvat, I., Tavitian, B., & Boisgard, R. (2015). Monitoring therapeutic efficacy of sunitinib using [18F]FDG and [18F]FMISO PET in an immunocompetent model of luminal B (HER2-positive)-type mammary carcinoma. *BMC Cancer*, *15*, 534(10pp).
12. Arvold, N. D., Heidari, P., Kunawudhi, A., Sequist, L. V., & Mahmood, U. (2015). Tumor hypoxia response after targeted therapy in EGFR-mutant non-small cell lung cancer. *Technol. Cancer Res. Treat*., *15*(2), 234–242.
13. Bruehlmeier, M., Kaser-Hotz, B., Achermann, R., Rohrer Bley, C., Wergin, M., Schubiger, P. A., & Ametamey, S. M. (2005). Measurement of tumor hypoxia in spontaneous canine sarcomas. *Vet. Radiol. Ultrasoun*., *46*(4), 348–354.
14. Kilian, K., Chabecki, B., Kiec, J., Kunka, A., Panas, B., Wójcik, M., & Pekal, A. (2014). Synthesis, quality control and determination of metallic impurities in 18F-fludeoxyglucose production process. *Rep. Pract. Oncol. Radiother*., *19*, 22–31.
15. Anzellotti, A., Bailey, J., Ferguson, D., McFarland, A., Bochev, P., Andreev, G., Awasthi, V., & Brown-Proctor, C. (2015). Automated production and quality testing of [18F]labeled radiotracers using the BG75 system. *J. Radioanal. Nucl. Chem*., *305*(2), 387–401.
16. Blom, E., & Koziorowski, J. (2014). Automated synthesis of [18F]FMISO on IBA Synthera®. *J. Radioanal. Nucl. Chem*., *299*(1), 265–270.
17. Nandy, S. K., & Rajan, M. (2010). Fully automated radiosynthesis of [18F]Fluoromisonidazole with single neutral alumina column purification: optimization of reaction parameters. *J. Radioanal. Nucl. Chem., 286*(1), 241–248.
18. Bowen, S. R., van der Kogel, A. J., Nordsmark, M., Bentzen, M. S., & Jeraj, R. (2011). Characterization of PET hypoxia tracer uptake and tissue oxygenation via electrochemical modeling. *Nucl. Med. Biol., 38*(6), 771–780.